

Ground state of the geometrically frustrated compound $\text{Tb}_2\text{Sn}_2\text{O}_7$

This article has been downloaded from IOPscience. Please scroll down to see the full text article.

2007 J. Phys.: Condens. Matter 19 446206

(<http://iopscience.iop.org/0953-8984/19/44/446206>)

View [the table of contents for this issue](#), or go to the [journal homepage](#) for more

Download details:

IP Address: 129.252.86.83

The article was downloaded on 29/05/2010 at 06:30

Please note that [terms and conditions apply](#).

Ground state of the geometrically frustrated compound $\text{Tb}_2\text{Sn}_2\text{O}_7$

Y Chapuis¹, A Yaouanc¹, P Dalmas de Réotier¹, S Pouget¹, P Fouquet²,
A Cervellino^{3,5} and A Forget⁴

¹ CEA/DSM/Département de Recherche Fondamentale sur la Matière Condensée,
F-38054 Grenoble, France

² Institut Laue-Langevin, Boite Postale 156X, F-38042 Grenoble Cedex 9, France

³ Laboratory for Neutron Scattering, ETH Zurich and Paul Scherrer Institut, CH-5232
Villigen-PSI, Switzerland

⁴ CEA/DSM/Département de Recherche sur l'Etat Condensé, les Atomes et les Molécules,
F-91191 Gif sur Yvette, France

Received 1 June 2007, in final form 14 September 2007

Published 16 October 2007

Online at stacks.iop.org/JPhysCM/19/446206

Abstract

Despite the observation of magnetic neutron reflections at low temperatures, muon-spin experiments have suggested the ground state of the geometrically frustrated magnetic material $\text{Tb}_2\text{Sn}_2\text{O}_7$ to be dynamical. This unique situation requires additional characterizations of this magnetic ground state. Here we report a neutron spin-echo investigation which supports the existence of a dynamical component in the ground state. This result is backed by a thorough analysis of the diffraction profiles. A physical model is put forward in which the energy splitting between the ground and first excited states of the Tb^{3+} ion is comparable to other energies present in this frustrated system.

(Some figures in this article are in colour only in the electronic version)

In many systems of physical interest, the configurations that minimize energy at the local level cannot propagate freely throughout space, due to constraints imposed by the nature of the interactions and the geometry of the lattice. This is a situation referred to as geometrical frustration. Examples are found in nature in different systems, including biological materials, some classes of liquid crystals and magnetic materials. Among the magnetic compounds, those crystallizing in the pyrochlore structure, a three-dimensional arrangement of corner-sharing tetrahedra, are of special interest because of the low connectivity of the structure and therefore the expected large degeneracy of their ground state. Examples of them are the $\text{R}_2\text{M}_2\text{O}_7$ insulators, where R is a rare-earth ion and $\text{M} = \text{Ti}$ or Sn . These have been the point of focus in recent years [1–3].

⁵ On leave from: CNR, Istituto di Cristallografia (CNR-IC), I-70126 Bari, Italy.

A near-universal consequence of geometrical frustration is the shift of the magnetic transition temperature of the system to a temperature much lower than would be expected based on the strength of the interactions. In addition, the ordered magnetic structure, if it exists, is usually non-collinear. $\text{Tb}_2\text{Sn}_2\text{O}_7$ is a typical case where, despite the large Curie–Weiss constant, $\theta_{\text{CW}} = -12$ K [4], the magnetic ordering occurs only at very low temperature. A non-collinear ordering appears at temperatures below the temperature $T_{\text{sh}} \simeq 0.88$ K at which a well-defined peak is seen in the specific heat [5]. The saturation value of the Tb^{3+} magnetic moment (μ_{Tb}) is $5.6(3) \mu_{\text{B}}$ [5, 6]. The magnetic reflections observed by neutron scattering are broader—and differently shaped—than the instrumental resolution function. The analysis of the nuclear specific heat suggests the ground state to be dynamical⁶. This is confirmed by muon-spin relaxation (μSR) experiments, which provide a timescale for the fluctuations: $\tau_{\mu} \simeq 10^{-10}$ s [6]. Later on, a second μSR work confirmed this picture qualitatively. However, the value of $\tau_{\mu} = 5 \times 10^{-9}$ s derived by Bert *et al* [7] from the analysis of the field dependence of λ_{Z} with the Redfield formula is dubious because λ_{Z} does not follow the field dependence predicted by that model [6].

That a magnetic ground state is dynamical and exhibits neutron magnetic reflections is by itself uncommon: it will be discussed further after the exposition of our new experimental results.

We shall present neutron spin-echo (NSE) measurements designed to study the spin dynamics of $\text{Tb}_2\text{Sn}_2\text{O}_7$, mainly below T_{sh} . In addition, we shall report a thorough analysis of the profiles of the magnetic reflections recorded at 0.11 K. These two sets of results will be discussed in relation to published data. Their implications concerning the magnetic properties of the $\text{Tb}_2\text{Sn}_2\text{O}_7$ ground state will be spelled out. In addition, in view of these results, we shall propose new studies for the two intriguing heavy fermion systems UPt_3 and URu_2Si_2 .

NSE gives access to the intermediate scattering function, $S(\mathbf{Q}, t)$, which carries information on both spatial and temporal spin correlations. It has been used intensively for the study of geometrically frustrated magnetic materials; see [8] and references therein. It is sensitive to fluctuating spins in the time range 10^{-11} – 10^{-8} s. The measurements were carried out with the IN11A spectrometer at the Institut Laue-Langevin (ILL), operating at a neutron wavelength of 5.5 Å (bandwidth 15%). The powder sample was the same as in [6]. It was cooled down using an ^3He insert installed in a so-called ILL orange cryostat. The data were taken in the temperature range $0.33 \text{ K} \leq T \leq 1.17 \text{ K}$.

Terbium stannate, $\text{Tb}_2\text{Sn}_2\text{O}_7$, is an insulator that crystallizes into the cubic space group $Fd\bar{3}m$ with the lattice parameter $a = 10.426(1) \text{ \AA}$ at room temperature and the free position parameter allowed by the space group for the 48f site occupied by oxygen, $x = 0.336$ [5, 6]. Powder neutron diffraction measurements have uncovered a magnetic structure with both ferromagnetic and antiferromagnetic components below $T_{\text{sr}} = 1.3(1) \text{ K}$, where non-liquid-like short-range magnetic correlations appear [5]. A steep increase in μ_{Tb} is observed on cooling in the vicinity of T_{sh} concomitantly with a narrowing of the magnetic reflections, which are still not resolution limited at low temperature [5, 6]. The magnetic structure adopted by $\text{Tb}_2\text{Sn}_2\text{O}_7$ implies a lowering of the space group symmetry, presumably due to a relatively strong magneto-elastic coupling. The tetragonal group $I4_1/amd$ was found to be consistent with the experimental data [5].

In figure 1 we display NSE spectra recorded for $T \leq 1.17 \text{ K}$. Quantitatively, the spectra for $T \geq 0.85 \text{ K}$ have been fitted to the sum of a stretched exponential and a constant term. This phenomenological approach provides a proper description of the data. It indicates a complex

⁶ The magnitude m_{eff} of the magnetic moment inferred from the nuclear specific heat, as quoted in [5], is erroneous. In fact, $m_{\text{eff}} = 4.5(4) \mu_{\text{B}}$. We thank P Bonville for a discussion on this matter.

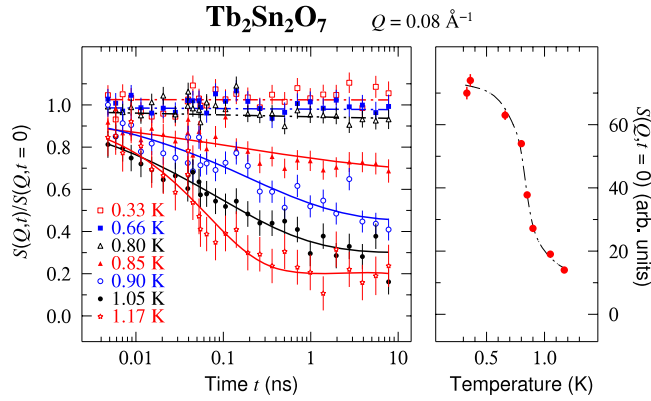


Figure 1. NSE results for $\text{Tb}_2\text{Sn}_2\text{O}_7$, at a momentum transfer $Q = 0.08 \text{ \AA}^{-1}$. Left-hand panel: spin-echo signals at various temperatures. The time window runs from 4×10^{-12} to 8×10^{-9} s. For temperatures greater or equal to 0.85 K, we plot as continuous lines the result of fits with $\tilde{S}(Q,t) = A\{\exp[-(t/\tau_{\text{NSE}})^\beta] - 1\} + 1$. $\tilde{S}(Q,t) \equiv S(Q,t)/S(Q,t=0)$, where $S(Q,t) = \int S(Q,\omega) \exp(i\omega t) d\omega$ is the dynamical magnetic structure factor. As indicated by polarization analysis (not shown here), for temperatures lower than 0.85 K, the neutron beam is slightly depolarized through the sample. The depolarization is of the order of a few per cent. The measured values of the $S(Q,t=0)$ points are consequently smaller than they should be, and so the deduced $\tilde{S}(Q,t)$ function is shifted upwards without changing its shape. The dashed-dotted lines are guides to the eye. We take heed of the instrumental resolution by dividing the signal from our sample by that of $\text{Ho}_{1.3}\text{Y}_{0.7}\text{Ti}_2\text{O}_7$, which is characterized by an elastic scattering (time-independent $S(Q,t)$) at low temperature. Right-hand panel: magnetic structure factor $S(Q,t=0)$ versus temperature. The half maximum amplitude is located near 0.85 K, whereas the temperature where we observe a well-defined peak in the specific heat is $T_{\text{sh}} = 0.88 \text{ K}$ [6]. The dashed-dotted line is a guide to the eye.

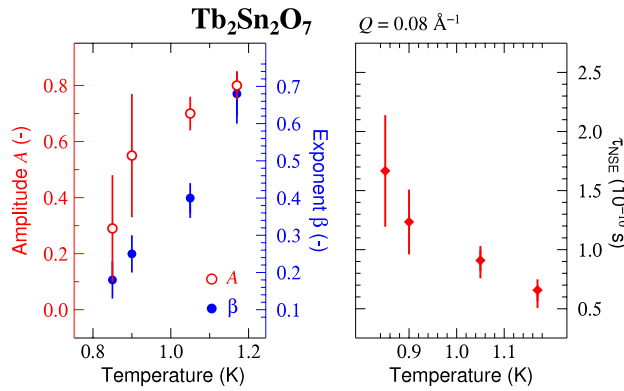


Figure 2. Fit parameters of the NSE signals versus temperature. Left-hand panel: the empty circles show the amplitude A and the filled one the exponent β . Right-hand panel: spin fluctuation time τ_{NSE} , as determined by NSE.

relaxation mechanism with more than one relaxation channel at play. The NSE experiment does not probe all of them. This justifies that the expression for $\tilde{S}(Q,t)$ does not vanish at large time in the NSE scale. As shown in figure 2, the fluctuation time deduced from the NSE measurements is in the range of 10^{-10} s. Even at 0.80 K, for which the magnetic reflections are intense, as gaged by $S(Q,t=0)$ (see figure 1), spin dynamics is still observed in the NSE

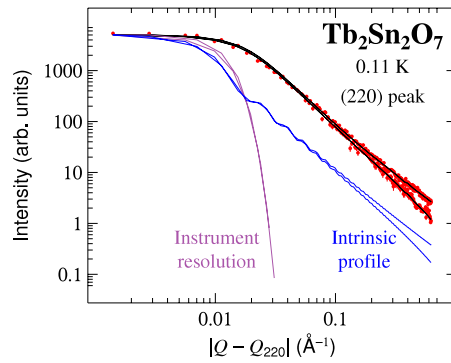


Figure 3. Profile of the (220) magnetic reflection obtained from the subtraction of diffraction patterns recorded at 0.11 and 1.23 K with neutrons of wavelength 2.453 \AA on a polycrystalline sample of $\text{Tb}_2\text{Sn}_2\text{O}_7$. The wavevectors Q and Q_{220} are expressed in \AA^{-1} . The different lines represent the instrument resolution, the intrinsic profile and the fit to the data that is obtained from a convolution of the latter two. The two data sets and associated profiles correspond to $Q - Q_{220}$ respectively positive and negative. The measured profile for $|Q - Q_{220}| > 0.03 \text{ \AA}^{-1}$ approximately follows a power law with an exponent ~ -1.8 : the (220) magnetic reflection, as well as the other reflections, have an approximately Lorentzian shape.

spectrum. From the slope displayed by the 0.80 K signal, the spin fluctuation time is estimated to be about $2(1) \times 10^{-10} \text{ s}$.

For $T < 0.80 \text{ K}$, no dynamics is evidenced by NSE. However, we shall show below that a careful analysis of the magnetic reflection profiles measured in powder diffraction is consistent with the presence of spin dynamics at lower temperature.

Our diffraction experiment performed at 100 K (not shown) indicates the atomic coherent domains to be very large, i.e. at least $1 \mu\text{m}$. The magnetic reflections are yet found to be much broader than the nuclear reflections, with Lorentzian-like heavy tails that are completely absent in the instrumental profile, which is a poly-Gaussian. The broadening in Q is found to be the same for the different magnetic reflections, which have been measured, i.e. from (111) to (511), by increasing the scattering angle. Figure 3 shows the profile of the (220) magnetic reflection.

A Lorentzian-like peak shape is a textbook indicator (see, for example, chapter 5 of [9]) of size broadening. However, that is not the only possibility, as we shall discuss later. Size, of course, refers to the ordered magnetic domains, which may well be smaller than the domains of atomic order. Therefore the magnetic reflections were fitted to a distribution of domain sizes, assuming the domains to be spherical and sharply defined. As a lattice is intrinsically discrete, a continuous size distribution is not very meaningful; it is a valid approximation only if the distribution varies very little over one lattice constant, and in this instance this is not so. Therefore we used a discretized distribution of radii R_k , with a constant step ΔR . The latter is chosen, with specific attention to the face-centered cubic lattice, as the smallest one that guarantees an integer number of cells in each k th sphere. As it turns out that $\Delta R < a$, the discretization is not coarse at all. The peak profiles corresponding to the different domain sizes were added together with weights given by the size distribution function, and subsequently convoluted with the instrument resolution function. In the experimental profile fit, we used comparatively the log-normal and gamma size distribution functions, which are appropriate for crystalline powders [10] and polycrystals [11], respectively. These both give similar results. Figure 3 presents the (220) peak profile description using the discretized gamma distribution shown in figure 4.

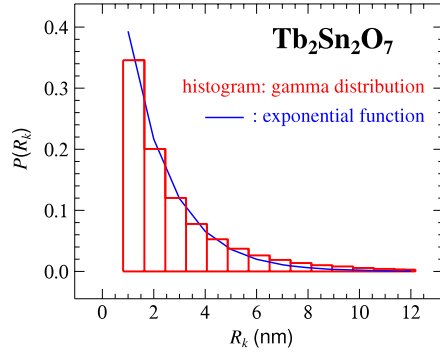


Figure 4. Size distribution $P(R_k)$ computed from measured profiles for $\text{Tb}_2\text{Sn}_2\text{O}_7$ versus the radius of the magnetic domains R_k . The computation has been performed assuming the gamma distribution, which is well-adapted to magnetic domains. This can be written $P(R_k) = R_k^{\alpha-1} \exp(-R_k/\theta) / [\theta^\alpha \Gamma(\alpha)]$, with $R_k = (k + 1/2) \Delta R$, $\Delta R = a(2\pi/3)^{-1/3}$ (where a is the lattice parameter), Γ the Gamma function, $\alpha = (R_a/\sigma_R)^2$ and $\theta = \sigma_R^2/R_a$ (where R_a is the average radius and σ_R its standard deviation). The best match to the experimental data is obtained with $R_a = 2.9$ (3) nm and $\sigma_R = 2.6$ (3) nm. The first size which is considered in the distribution is R_1 , since R_0 is unrealistic ($R_0 < a$). $P(R_k)$ is well approximated by an exponential distribution (full line) proportional to $\exp(-R_k/U)$ with a decay length $U = 1.68$ nm.

In general, the maximum of $P(R_k)$ gives the most frequent domain size [12]. As seen in figure 4, our distribution decreases monotonously with the domain size and it is well approximated by an exponential, with maximum at zero size. Similar remarks hold for the log-normal distribution (not shown). Remarkably, the most frequent domains would contain just a few spins. This is not understandable in the static picture, where domain size should be a consequence of the interplay of surface and volume magnetic energies. This suggests that the observed line broadening results from quasi-elastic scattering. In this framework, assuming a linear energy–momentum dispersion, we tentatively estimate a bound on the characteristic scattering timescale τ_{sc} . For a given reflection, we denote \mathbf{K}_f as the wavevector of the elastically scattered beam and $\Delta\mathbf{K}_f$ as the change in wavevector resulting from the quasi-elastic process. The broadening arises because the scattered neutrons wavevectors are spread, with a width $\Delta\mathbf{K}_f$. With our notation, the change in energy during the scattering is written as $\Delta E = [\hbar^2/(2m_n)][(\mathbf{K}_f + \Delta\mathbf{K}_f)^2 - \mathbf{K}_f^2] \simeq [\hbar^2/(2m_n)]2K_f\Delta K_f \cos\phi$, where m_n is the neutron mass and ϕ is the angle between \mathbf{K}_f and $\Delta\mathbf{K}_f$. Previously, the $2K_f\Delta K_f \cos\phi$ term rather than $(\Delta\mathbf{K}_f)^2$ was neglected [6]. Since $\Delta K_f = \Delta Q/\sin\phi$, where ΔQ measures the half-width at half maximum of the intrinsic peak profile ($\Delta Q = 0.0075 \text{ \AA}^{-1}$; see figure 3), an order of magnitude for the change in energy of a neutron during the scattering process is evaluated to be $80 \mu\text{eV}$.⁷ Using the energy–time Heisenberg uncertainty relation, we then get a bound for the spin fluctuation time $\tau_{\text{sc}} \gtrsim 8 \times 10^{-12}$ s. The constant Q -width results probably from an approximately isotropic distribution of $\Delta\mathbf{K}_f$.

In conclusion, NSE, neutron diffraction, μSR and the nuclear specific heat measurements all point to a dynamical \mathbf{Q} -component in the ground state of $\text{Tb}_2\text{Sn}_2\text{O}_7$ at low temperature with a timescale in the 10^{-10} s range. We recall that the field at the muon site, \mathbf{B}_{loc} , is expressed as a weighted sum of Fourier components of μ_{Tb} ; see e.g. equation A13 in [13]. The non-observation of a μSR Larmor precession frequency reflects the overwhelming contribution of

⁷ This order of magnitude is calculated for $\phi = \pi/4$, the scattering geometry for which $\phi = 0$ does not indeed contribute to the reflection broadening.

the dynamical \mathbf{Q} -component in \mathbf{B}_{loc} . The μSR data rule out a picture which would assume the compound to be spatially inhomogeneous, for example made of conventional ordered domains mixed with paramagnetic domains.

The number of compounds for which neutron magnetic reflections are observed while a defined μSR signature of a phase transition temperature is not detected is extremely restricted. To the best of our knowledge, only UPt_3 [14, 15]⁸, URu_2Si_2 [16, 17] and $\text{Er}_2\text{Ti}_2\text{O}_7$ [18, 19] have these properties. We should discard the last compound, at least for the time being, since it is still unknown if symmetry arguments cannot explain the vanishing of \mathbf{B}_{loc} . Interestingly, it is known that UPt_3 and URu_2Si_2 display Lorentzian magnetic reflections [20]. An analysis of the profile of these reflections along the lines of this report would be worthwhile.

Why is $\text{Tb}_2\text{Sn}_2\text{O}_7$ so special? We first note that the crystal field of the Tb^{3+} ions in $\text{Tb}_2\text{Ti}_2\text{O}_7$ at low energy has a doublet–doublet structure [21]. Since $\text{Tb}_2\text{Sn}_2\text{O}_7$ crystallizes in the same space group in its paramagnetic phase, the same structure is expected. Guided by the differences in the quadrupole splitting as measured by ^{155}Gd Mössbauer spectroscopy [22], we estimate the doublet–doublet splitting is reduced by no more than $\sim 30\%$ in the stannate relative to the titanate, i.e. a splitting of at least 13 K is computed for $\text{Tb}_2\text{Sn}_2\text{O}_7$. Therefore, at sufficiently low temperature the magnetic properties are, to a good approximation, determined by the ground-state doublet. As pointed out earlier, a lowering of the space group symmetry has been observed at low temperature. This leads to a splitting of the ground-state doublet which seems to be of the order of 1.5 K [5]. Because of the breaking of time-reversal symmetry below T_{sh} , the ground state is magnetic. We compute $\mu_{\text{Tb}} = g_J \mu_B \langle +|J_z|+ \rangle f(\delta/a_Z)$, where $g_J = 3/2$ is the Landé factor, $|+ \rangle$ is one of the doublet wavefunctions and $f(\delta/a_Z)$ is a function that depends on the ratio of the crystal field splitting, δ , to the Zeeman energy arising from the molecular field, a_Z . By definition, $f(0) = 1$, and it decreases monotonously with δ/a_Z . Interestingly, a recent expression of $|+ \rangle$ [23] leads to $g_J \langle +|J_z|+ \rangle \simeq 5.5$, whereas we compute $g_J \langle +|J_z|+ \rangle \simeq 4.5$ for another proposed wavefunction [24]. From estimates of δ and a_Z , we deduce $f > 0.9$. Hence the former wavefunction is consistent with the experimental estimate of μ_{Tb} . We speculate that the fluctuations observed in $\text{Tb}_2\text{Sn}_2\text{O}_7$ below T_{sh} are induced by transitions between the ground and first excited states resulting from the degeneracy lifting.

In summary, we have presented neutron scattering data that support the existence of a dynamical component in the ground state in $\text{Tb}_2\text{Sn}_2\text{O}_7$. In addition, we have sketched a physical model that can explain this observed dynamical character. The Tb^{3+} ground-state doublet is split into two singlets separated by an energy of the order of the effective interaction energy [25] accounting for the exchange and dipole interactions. This suggests that the dynamics arises from transitions between the ground and first excited states. To put the model on a firmer ground, a detailed investigation of the crystal field would be welcome, as well as a detailed theoretical study.

Acknowledgments

We are grateful to S T Bramwell, G Ehlers and J Lago for the possibility of using their $\text{Ho}_{1.3}\text{Y}_{0.7}\text{Ti}_2\text{O}_7$ sample that enabled us to determine the instrumental resolution of the IN11A spin-echo spectrometer. We thank B Fåk for drawing our attention to the Lorentzian shape of the magnetic reflections in UPt_3 and URu_2Si_2 , and S H Curnoe and P C M Gubbens for discussions on symmetry and crystal fields.

⁸ No signature of the magnetic order has been observed by nuclear magnetic resonance (NMR) in UPt_3 [26] either.

References

- [1] Ramirez A P 2001 *Handbook of Magnetic Materials* vol 13, ed K H J Buschow (Amsterdam: Elsevier)
- [2] Diep H T (ed) 2004 *Frustrated Spin Systems* (Singapore: World Scientific)
- [3] Moessner R and Ramirez A P 2006 *Phys. Today* (February) **24–9**
- [4] Matsuhira K, Hinatsu Y, Tenya K, Amitsuka H and Sakakibara T 2002 *J. Phys. Soc. Japan* **71** 1576
- [5] Mirebeau I, Apetrei A, Rodríguez-Carvajal J, Bonville P, Forget A, Colson D, Glazkov V, Sanchez J P, Isnard O and Suard E 2005 *Phys. Rev. Lett.* **94** 246402
- [6] Dalmas de Réotier P et al 2006 *Phys. Rev. Lett.* **96** 127202
- [7] Bert F, Mendels P, Olariu A, Blanchard N, Collin G, Amato A, Baines C and Hillier A D 2006 *Phys. Rev. Lett.* **97** 117203
- [8] Ehlers G 2006 *J. Phys.: Condens. Matter* **18** R231
- [9] Giacovazzo C, Monaco H L, Artioli G, Viterbo D, Ferraris G, Gilli G, Zanotti G and Catti M 2002 *Fundamentals of Crystallography* (Oxford: Oxford University Press)
- [10] Kiss L F, Söderlund J, Niklasson G A and Granqvist C G 1999 *Nanotechnology* **10** 25
- [11] Yu H, Liu G and Song X 1998 *Mater. Mater. Trans. A* **29** 3081
- [12] Popa N C and Balzar D 2002 *J. Appl. Crystallogr.* **35** 338
- [13] Dalmas de Réotier P and Yaouanc A 1997 *J. Phys.: Condens. Matter* **9** 9113
- [14] Aeppli G, Bucher E, Broholm C, Kjems J K, Baumann J and Hufnagl J 1988 *Phys. Rev. Lett.* **60** 615
- [15] Dalmas de Réotier P, Huxley A, Yaouanc A, Flouquet J, Bonville P, Imbert P, Pari P, Gubbens P C M and Mulders A M 1995 *Phys. Lett. A* **205** 239
- [16] Broholm C, Kjems J K, Buyers W J L, Matthews P, Palstra T T M, Menovsky A A and Mydosh J A 1997 *Phys. Rev. Lett.* **58** 1467
- [17] Yaouanc A, Dalmas de Réotier P, Huxley A D, Bonville P, Gubbens P C M, Mulders A M, Lejay P and Kuni S 1997 *Physica B* **230–232** 269
- [18] Champion J D M et al 2003 *Phys. Rev. B* **68** 020401(R)
- [19] Lago J, Lancaster T, Blundell S J, Bramwell S T, Pratt F L, Shirai M and Baines C 2005 *J. Phys.: Condens. Matter* **17** 979
- [20] van Dijk N H, Rodière P, Yakhov F, Fernández-Díaz M-T, Fåk B, Huxley A and Flouquet J 2001 *Phys. Rev. B* **63** 104426
- [21] Gingras M J P, den Hertog B C, Faucher M, Gardner J S, Dunsiger S R, Chang L J, Gaulin B D, Raju N P and Greedan J E 2000 *Phys. Rev. B* **62** 6496
- [22] Bonville P, Hodges J A, Ocio M, Sanchez J P, Vulliet P, Sosin S and Braithwaite D 2003 *J. Phys.: Condens. Matter* **15** 7777
- [23] Curnoe S H 2007 *Phys. Rev. B* **75** 212404
- [24] Molavian H R, Gingras M J P and Canals B 2007 *Phys. Rev. Lett.* **98** 157204
- [25] den Hertog B C and Gingras M J P 2000 *Phys. Rev. Lett.* **84** 3430
- [26] Tou H, Kitaoka Y, Asayama K, Kimura N, Ōnuki Y, Yamamoto E and Maezawa K 1996 *Phys. Rev. Lett.* **77** 1374